energies

MDPI

Article

Kinetic and Thermodynamic Analysis of High-Pressure CO_2 Capture Using Ethylenediamine: Experimental Study and Modeling

Josselyne A. Villarroel, Alex Palma-Cando, Alfredo Viloria and Marvin Ricaurte *

Grupo de Investigación Aplicada en Materiales y Procesos (GIAMP), School of Chemical Sciences and Engineering, Yachay Tech University, Hda. San José s/n y Proyecto Yachay, Urcuquí 100119, Ecuador; josselyne.villarroel@yachaytech.edu.ec (J.A.V.); apalma@yachaytech.edu.ec (A.P.-C.); dviloria@yachaytech.edu.ec (A.V.)

* Correspondence: mricaurte@yachaytech.edu.ec

Abstract: One of the alternatives to reduce CO_2 emissions from industrial sources (mainly the oil and gas industry) is CO_2 capture. Absorption with chemical solvents (alkanolamines in aqueous solutions) is the most widely used conventional technology for CO_2 capture. Despite the competitive advantages of chemical solvents, the technological challenge in improving the absorption process is to apply alternative solvents, reducing energy demand and increasing the CO_2 captured per unit of solvent mass. This work presents an experimental study related to the kinetic and thermodynamic analysis of high-pressure CO_2 capture using ethylenediamine (EDA) as a chemical solvent. EDA has two amine groups that can increase the CO_2 capture capacity per unit of solvent. A non-stirred experimental setup was installed and commissioned for CO_2 capture testing. Tests of the solubility of CO_2 in water were carried out to validate the experimental setup. CO_2 capture testing was accomplished using EDA in aqueous solutions (0, 5, 10, and 20 wt.% in amine). Finally, a kinetic model involving two steps was proposed, including a rapid absorption step and a slow diffusion step. EDA accelerated the CO_2 capture performance. Sudden temperature increases were observed during the initial minutes. The CO_2 capture was triggered after the absorption of a minimal amount of CO_2 (~10 mmol) into the liquid solutions, and could correspond to the "lean amine acid gas loading" in a typical sweetening process using alkanolamines. At equilibrium, there was a linear relationship between the CO_2 loading and the EDA concentration. The CO_2 capture behavior obtained adapts accurately (AAD < 1%) to the kinetic mechanism.

Keywords: high-pressure system; CO_2 capture; ethylenediamine; kinetics; thermodynamic analysis; modeling

Citation: Villarroel, J.A.; Palma-Cando, A.; Viloria, A.; Ricaurte, M. Kinetic and Thermodynamic Analysis of High-Pressure CO_2 Capture Using Ethylenediamine: Experimental Study and Modeling. *Energies* **2021**, *14*, 6822. https://doi.org/10.3390/en14206822

Academic Editor: João Fernando Pereira Gomes

Received: 6 September 2021
Accepted: 27 September 2021
Published: 19 October 2021

1. Introduction

CO_2 is a greenhouse gas that has a high impact on atmospheric pollution. In 2020, the global CO_2 emissions were estimated at 30.6 Gt [1], and sustained growth (approximately 0.43 Gt/y) is expected until 2040 [2]. Reducing CO_2 emissions is one of the Paris Agreement's goals [3] to offset the trend. Therefore, it is necessary to make technological and economic efforts worldwide to achieve this goal. The application of carbon capture and storage (CCS) technologies is an alternative for reducing CO_2 emissions from industrial sources—mainly the oil and gas industry [4].

Conventional technologies based on chemical absorption, physical absorption, and membranes are commonly used for CO_2 capture. In particular, "amine-based chemical absorption appears to be the most technologically mature and commercially viable method" [5], because it allows CO_2 capture at a large scale. Chemical absorption is a centralized process consisting of an absorption column where the CO_2-containing gas (e.g., natural gas, flue gas, or fuel gas) comes into contact with a chemical solvent, whereupon

chemical reactions take place with the CO_2 molecules. The chemical solvent is then regenerated by heat in a stripping tower, and it is returned to the absorption column. The typical process design criteria for the chemical absorption process are the amine type and concentrations, solution flowrate, the absorber and stripper types (tray or packed), absorber and stripper heights and diameters, and the thermal duties (heating and cooling) of all heat transfer equipment [6]. This process requires high capital expenses (high CAPEX) but low operational expenditures (low OPEX) due to solvent regeneration [7,8].

Alkanolamines in aqueous solutions are widely used as chemical solvents for CO_2 capture, with monoethanolamine (MEA) being the most popular [9,10]. The typical concentration used in chemical solvents (10–65 wt.% in amine) depends mainly on the alkanolamine characteristics, e.g., CO_2 absorption capacity, physical properties, and thermal stability. Chemical solvents can capture up to 99% of the CO_2 from a gas stream [11]. Despite the competitive advantages of chemical solvents, the technological challenge lies in identifying and applying new or reformulated solvents to reduce the energy demand and increase the CO_2 captured per unit of solvent mass [12–14].

Alternative chemical solvents can be proposed from amines other than alkanolamines [15,16]. Ethylenediamine (EDA) is the first member of the so-called "polyethylene amines". A competitive advantage of EDA over alkanolamines is low corrosivity [17]. EDA has an amino group at the end of each molecule, so it is expected that the double amino group could increase the CO_2 capture capacity per unit of solvent. Li et al. [18] and Salvi et al. [19] carried out kinetic studies of CO_2 capture using EDA. Zhou et al. [20] worked with EDA to propose CO_2 capture at high concentrations (>30 wt.% in amine). To our understanding, the double amino group that EDA possesses does not benefit from these concentrations, due to the relative abundance of nitrogen in the EDA molecule (46.59%) compared to the MEA molecule (22.65%) for CO_2 capture applications. Hafizi et al. [21], Kumar et al. [22], and Nakhjiri and Heydarinasab [23] reported the use of EDA as an additive to improve CO_2 capture processes. Ciftja et al. [24], da Silva and Svendsen [25], and Thompson et al. [26] analyzed the chemical reaction mechanisms of EDA in CO_2 absorption processes. At atmospheric pressure, the primary reaction between carbon dioxide and ethylenediamine in an aqueous solution is:

$$CO_2 + H_2N(CH_2)_2NH_2 \rightleftharpoons {}^{+}H_3N(CH_2)_2NHCOO^{-} \quad (1)$$

resulting in the formation of 2-ammonioethylcarbamate [27,28]. A side reaction of

$$2CO_2 + 2H_2N(CH_2)_2NH_2 \rightleftharpoons {}^{-}OOCHN(CH_2)_2NHCOO^{-} + {}^{+}H_3N(CH_2)_2NH_3^{+} \quad (2)$$

might take place, resulting in an intramolecular disalt. However, this reaction does not occur to a high extent, resulting in an insignificant contribution to the reaction rate [29]. The same behavior has been observed for CO_2 and EDA reactions under high-pressure conditions, mainly yielding 2-ammonioethylcarbamate [30].

According to the damping-film theory [31,32], the relationship between partial pressure of the gas and time can be described for the isothermal absorption of gas, as follows:

$$ln\frac{P_o - P_e}{P - P_e} = ut \quad (3)$$

where P represents the instantaneous CO_2 partial pressure, P_o and P_e denote partial pressure at the starting and at equilibrium conditions, respectively, u stands for the apparent absorption rate constant, and t is the time. By applying an equation of state for a real gas, the last equation can be written in terms of CO_2 mole numbers as follows:

$$ln\frac{n_o - n_e}{n - n_e} = kt \quad (4)$$

where k is also the apparent absorption rate constant. The natural logarithm of the relationship between CO_2 mole numbers in the gas phase is directly proportional to the time passed during the absorption process. Thus, the constant rate k can be used to determine the apparent absorption rate performance of an aqueous EDA solution at different concentrations.

CO_2 capture using chemical solvents under high-pressure conditions is a typical process in the oil and gas industry—specifically, in natural gas processing operations—to meet quality specifications or reduce operational problems due to the presence of CO_2 in pipelines and equipment [33]. Many studies of CO_2 capture at the laboratory scale are carried out to improve and identify new solvents; however, many of them are performed in low-pressure experimental systems, and their results could differ significantly from those obtained in high-pressure systems. To the best of our knowledge, an integrated study focused on the kinetics and thermodynamics of CO_2 capture using EDA in aqueous solutions has not been reported using high-pressure systems. In this work, an experimental study is presented that aims to delve into the kinetic and thermodynamic analysis of the high-pressure CO_2 capture process using EDA. A non-stirred experimental setup was installed and commissioned for CO_2 capture testing, with the main distinction being the pure CO_2 bubbling directly into the liquid phase to promote the initial mass transfer through the gas–liquid interface. In the first stage, tests of the solubility of CO_2 in water were carried out to validate both the experimental setup and the proposed methodology. Afterwards, CO_2 capture testing was performed using EDA in aqueous solutions at different concentrations. Some parameters—time-dependent and under equilibrium conditions—were defined in order to study the kinetic and thermodynamic behavior of the CO_2 capture process. Finally, a kinetic model that allows for the determination of the CO_2 loading vs. time and the apparent absorption rate performance was proposed.

2. Methods

2.1. Materials

Carbon dioxide (purity > 99.995%) was supplied by Swissgas (Quito, Ecuador). Ethylenediamine (CAS number 107-15-3, purity $\geq$ 98.5%) was purchased from Sigma-Aldrich. Ultrapure water (resistivity = 18.2 MΩ.cm) produced by a laboratory water purification system from Merck Millipore was used to prepare the aqueous amine solutions.

2.2. Experimental Setup

The experimental setup used for the high-pressure CO_2 capture experiments is schematically depicted in Figure 1; it consists of a non-stirred pressure vessel (Parr Instrument Co., Moline, USA, model 4763) made of alloy C-276 with an internal volume of 98.7 cm^3. The vessel has a movable head equipped with: (1) a differential pressure gauge, (2) a 0–20,685 KPa pressure transducer with an accuracy of ±10 KPa, (3) a type J thermocouple accurate to within ±0.1 K, and (4) a valve series allowing gas release, liquid sampling, and gas injection into the liquid phase. A pressure regulator connected to a pure CO_2 store cylinder is used for the gas supply. A heating unit and a temperature controller (Parr Instrument Co., model 4838) are used to control the vessel temperature. The setup is connected to a data acquisition interface, which records temperature and pressure measurements on a computer using SpecView 32 SCADA software (SpecView Corp., Gig Harbor, WA, USA). The vessel pressurization was carried out in a pulse by bubbling the pure CO_2 directly into the liquid phase to guarantee an intimate contact between the gas and the liquid from the experiments' first instants. This action could represent an advantage in the initial gas mass transfer process through the gas–liquid interface [34,35], considering that it is a non-stirred system.

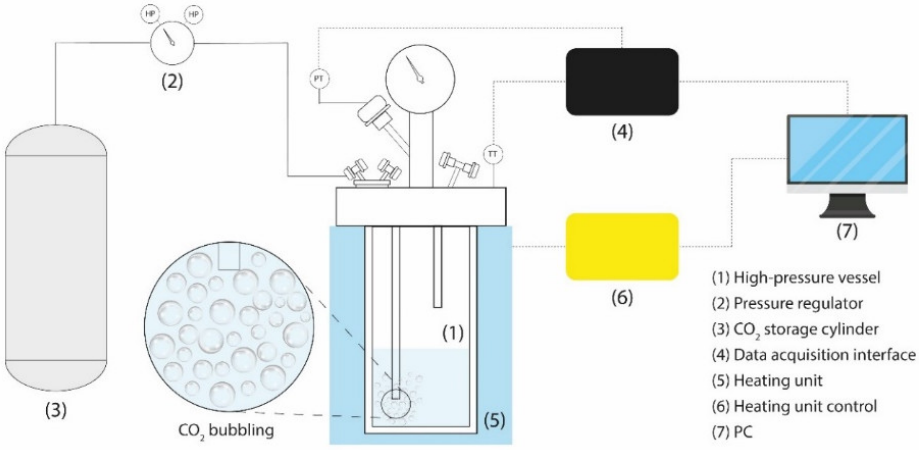

Figure 1. Schematic diagram of the high-pressure setup.

The experimental setup is designed to work in extreme conditions, i.e., maximum allowable working pressure (MAWP) 20,685 KPa, and maximum temperature 500 K. For safety reasons, the maximum allowable operating pressure (MAOP) was reduced to 6900 KPa.

2.3. CO_2 Solubility Testing Procedure

Testing of the solubility of CO_2 in water was performed to validate the high-pressure experimental setup by measuring the high-pressure vessel's equilibrium pressure for a known amount of gas and water in a closed system (batch mode). Initially, the high-pressure vessel was charged with 30 ± 0.2 cm^3 of ultrapure water using a glass pipette. The vessel was coupled to the experimental setup, and the temperature was set to 303 K. Then, the vessel was pressurized with pure CO_2 up to the desired initial pressure value (700, 2100, 3500 KPa), and the system was closed. Pressure and temperature data were recorded until pressure stabilization for 24 h.

2.4. CO_2 Capture Testing Procedure Using EDA

The ethylenediamine aqueous solutions were prepared at different concentrations (0, 5, 10, and 20 wt.% in amine) by adding the appropriate amine mass to ultrapure water while stirring it for 1 min. The experimental procedure defined for CO_2 capture testing using EDA was similar to that developed for the CO_2 solubility tests. The high-pressure vessel was loaded with 30 ± 0.2 cm^3 of the aqueous EDA solution to be tested. The vessel was coupled to the experimental setup, and the temperature was set to 303 K. The vessel was then pressurized with pure CO_2 up to 3500 KPa, and the system was closed. The initial pressure (3500 KPa) was established to maximize the driving force of the CO_2 capture process [15]. Pressure and temperature data were recorded until pressure stabilization for 12 h.

2.5. Data Processing

The pressure and temperature data as a function of time obtained during the experiments were used for the kinetic and thermodynamic analysis of the high-pressure CO_2 capture process. The analysis was based on quantifying the variability of the gas phase moles. Two main parameters were defined:

- *The quantity of CO_2 removed* refers to the gaseous phase moles transferred to the liquid phase, with respect to the initial amount of gas loaded into the high-pressure vessel. This quantity was calculated using Equation (5):

$$CO_{2_{removed}}|_t = n_{gas}\Big|_{t_o} - n_{gas}\Big|_t = \frac{PV}{zRT}\Big|_{t_o} - \frac{PV}{zRT}\Big|_t \quad (5)$$

where n_{gas} is the CO_2 mole number in the gas phase, P is the vessel pressure, V is the gas phase volume, z is the compressibility factor calculated by the Peng–Robinson equation of state [36], and T is the vessel temperature. Moreover, t_o and t are the initial time and an instantaneous time of the experiment, respectively.

- *The CO_2 loading* refers to the amount of CO_2 removed from the gas phase for each liquid (amine + water) mole initially introduced into the high-pressure vessel. The CO_2 loading was calculated using Equation (6):

$$CO_{2_{loading}}\Big|_t = \frac{CO_{2_{removed}}|_t}{n_{liquid}} \quad (6)$$

where n_{liquid} is the initial number of moles in the liquid phase. Appendix A shows the number of moles in each solution for the different amine concentrations used in this study. For this calculation, the experimental density data of aqueous EDA solutions at 303 K reported by Egorov et al. [37] were used.

Furthermore, the following additional time-dependent parameters were defined to compare the CO_2 capture process kinetics:

- t_{25}, t_{50}, and t_{90} refer to the time required to reach 25%, 50%, and 90%, respectively, of the total amount of CO_2 removed from the gas phase at the end of each experiment.
- dn/dt refers to the CO_2 capture rate. This was calculated directly on the curve of the removed amount of CO_2 from the gas as a function of time, and corresponds to the maximum value of gas consumption in the experiments' first instants. This value was obtained numerically using the initial slope method [38].

3. Results and Discussion

3.1. CO_2 Solubility Testing

Figure 2 shows the typical curves obtained during the CO_2 solubility tests. Figure 2a represents the drop in pressure as a function of time, where the pressure stabilization was achieved in the first 3 h. The final pressure reached corresponds to the equilibrium pressure at the conditions of CO_2 saturation in water, since these values were close to the equilibrium pressure estimated by the semi-empirical model of CO_2 solubility proposed by Ricaurte et al. [39] applied to each initial pressure studied (700, 2100, 3500 KPa). Figure 2b shows the CO_2 removed from the gas phase as a function of time. The amount of CO_2 solubilized into the water was proportional to the initial pressure, due to a higher driving force. The CO_2 solubility tests indicated that it is possible in non-stirred systems to achieve pressure stabilization in short times (<4 h), up until equilibrium conditions are reached in the saturation of CO_2 into water. In contrast, Farajzadeh et al. [40] reported pressure stabilization for a time >48 h in high-pressure CO_2 solubilization tests in quiescent conditions. Our experimental system's main distinction was the initial bubbling of CO_2 into the liquid solution, significantly reducing the time required for liquid saturation in non-stirred experimental setups [41].

Table 1 summarizes the kinetic and thermodynamic data obtained from the CO_2 solubility tests. The CO_2 capture rate (dn/dt) was increased at a higher initial pressure. For the most suitable case ($P_o = 3500$ KPa), the t_{25}, t_{50}, and t_{90} values corresponded to 2.20 min, 23.31 min, and 145.30 min, respectively. For the other initial pressures, 90% of the CO_2 was captured in ~180 min. The CO_2 loading in each experiment was consistent with the reference data of CO_2's solubility in water [39]. Therefore, the CO_2 solubility tests showed that (a) the experimental setup was suitable for carrying out CO_2 capture studies where equilibrium conditions are reached in <4 h, and (b) at a higher initial pressure, a greater driving force was obtained for the CO_2 capture process, maximizing the CO_2 loading at the equilibrium conditions. For these reasons, the CO_2 capture tests using the EDA were carried out at the highest initial pressure.

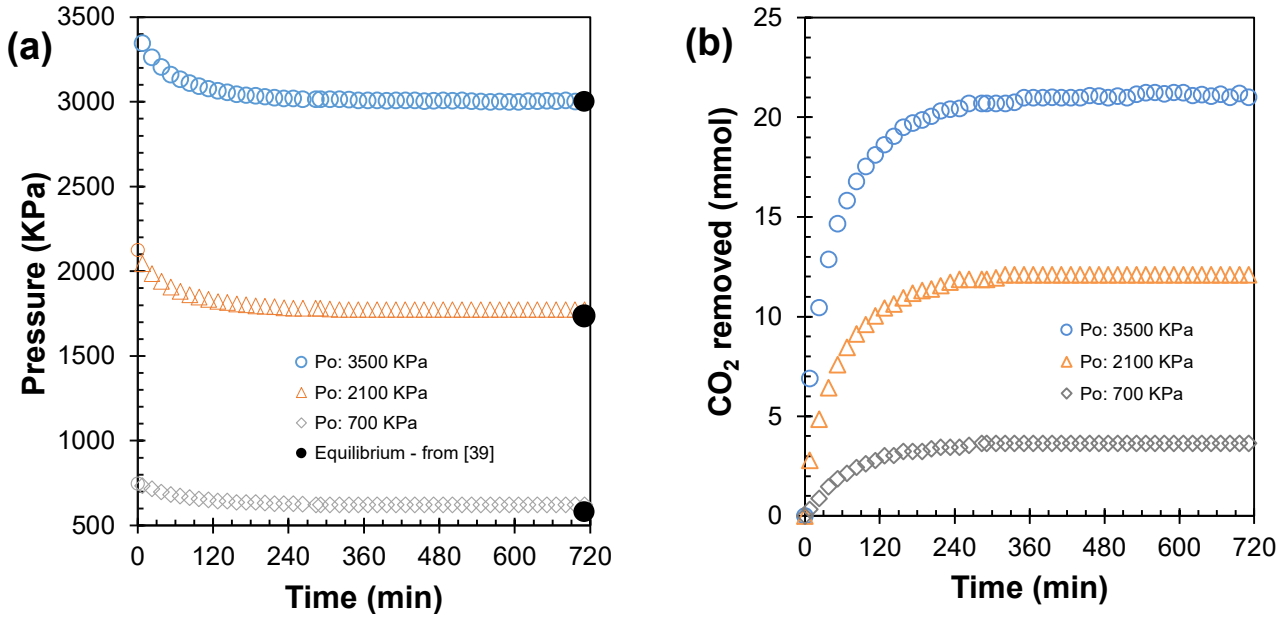

Figure 2. CO_2 solubility testing: (**a**) pressure vs. time; (**b**) CO_2 removed vs. time.

Table 1. CO_2 solubility testing: Kinetic and thermodynamic data.

Kinetic Data						Thermodynamic Data		
P_o (KPa)	dn/dt (mmol/min)	t_{25} (min)	t_{50} (min)	t_{90} (min)	P_{final} (KPa)	CO_2 Removed (mmol)	CO_2 Loading (*) (mmol CO_2/mol H_2O)	CO_2 Solubility (**) (mmol CO_2/mol H_2O)
700	0.034	24.52	45.04	192.55	623	3.64	2.20	2.39
2100	0.189	8.87	32.43	167.90	1774	12.10	7.30	7.57
3500	0.654	2.20	23.31	145.30	3007	21.25	12.82	12.89

(*) Moles of H_2O: 1.660; (**) calculated from [39].

3.2. CO_2 Capture Testing Using EDA

Figure 3 shows the characteristic curves obtained during the CO_2 capture testing using EDA. Figure 3a depicts the drop in pressure as a function of time. The drop in pressure was proportional to the amine concentration. For the 20 wt.% amine solution, the gas consumption represented a pressure drop of ~50% from the initial pressure. Figure 3b shows the temperature profile in the first 5 min of the CO_2 capture process, where a "sudden" temperature increase was observed in the initial moments of the CO_2–liquid solution contact. The highest temperature points were reached approximately one minute after the CO_2 pressurization, being proportional to the amine concentration. The maximum value reached was ~324 K for the 20 wt.% amine solution, representing a $\Delta T = 21\ K$. The temperature increments were related to the exothermic reaction between the CO_2 and the aqueous EDA solutions. Similar behavior was observed in the absorption processes of CO_2 [42] and other gases [43] in aqueous amine solutions. This exothermic phenomenon must be considered in the design of absorption towers for CO_2 capture using amines, since "one of the most important considerations involved in designing gas absorption towers is to determine whether temperatures will vary along with the height of the tower due to heat effects; note that the solubility usually depends strongly on temperature" [44]. A more detailed analysis of the exothermicity effect is presented in Section 3.3.

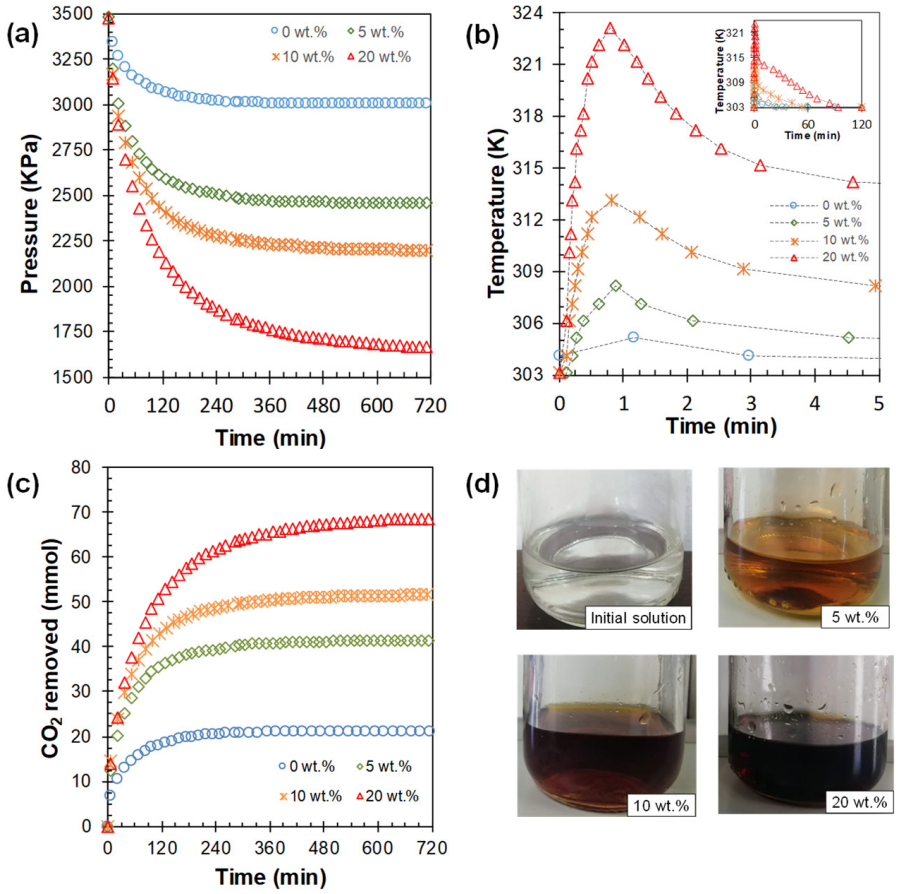

Figure 3. CO_2 capture using EDA: (**a**) pressure vs. time; (**b**) temperature vs. time; (**c**) CO_2 removed vs. time; (**d**) snapshots of aqueous amine solutions at the end of the experiments.

Figure 3c shows the CO_2 removed as a function of time. The amount of CO_2 captured was proportional to the concentration of the amine solution due to the EDA–CO_2 chemical affinity. Kumar et al. [22] proposed the use of EDA as an activator in the CO_2 capture process by increasing the solubility capacity of CO_2 in the amine aqueous solutions (chemical solvents). Snapshots of the aqueous amine solutions were taken at the end of the experiments (see Figure 3d). An increase in the intensity of a yellowish-brown color (amber color) could be observed with the naked eye in the aqueous amine solutions. The variability in the color intensity was proportional to the amine concentration, which correlates with the amount of CO_2 captured.

Table 2 summarizes the kinetic and thermodynamic data obtained from the CO_2 capture testing using EDA. The CO_2 capture rate (dn/dt) varied with the EDA concentration, obtaining the highest rate at 10 wt.%. Surprisingly, at the 20 wt.% amine concentration, the CO_2 capture rate was the lowest, but the CO_2 removed from the gas phase at equilibrium was the highest. A higher amine concentration increases the viscosity of aqueous amine solutions, unfavorably affecting the CO_2 mass transfer rates [20,45]. Moreover, at 20 wt.% amine concentration, there was a more significant temperature increase in the liquid solution (see Figure 3b), which might directly affect the CO_2 capture kinetics. Fan et al. [46] reported a decrease in the CO_2 capture rate using alkanolamine aqueous solutions (e.g., MEA and diethanolamine (DEA)) with temperature increases. In all of the EDA aqueous solutions studied, the t_{90} parameter was less than 300 min (<5 h). The time required for CO_2 capture can be reduced in stirred experimental setups or continuous processes at different scales, i.e., pilot-plant-scale [47–49] or large-scale [50–52]. The CO_2 removed and the CO_2 loading were proportional to the amine concentration at equilibrium conditions, so with the increase in the concentration of EDA in the liquid solution, there was a corresponding

increase in the CO_2 solubility and, subsequently, the EDA–CO_2 chemical reaction took place, increasing the CO_2 loading.

Table 2. CO_2 capture using EDA: Kinetic and thermodynamic data.

	Kinetic Data					Thermodynamic Data	
EDA Conc. (wt.%)	***dn/dt* (mmol/min)**	**t_{25} (min)**	**t_{50} (min)**	**t_{90} (min)**	**P_{final} (KPa)**	**CO_2 Removed (mmol)**	**CO_2 Loading (*) (mmol CO_2 /mol Liquid)**
0	0.654	2.20	23.31	145.30	3007	21.25	12.82
5	0.974	4.35	24.23	155.11	2450	41.63	26.03
10	1.040	5.28	27.28	172.16	2195	51.81	33.66
20	0.859	11.55	44.56	255.91	1640	69.72	49.03

(*) Initial moles of liquid: see Appendix A.

3.3. CO_2 Capture Using EDA: Reaction Exothermicity Effects

Figure 4 shows the pressure behavior (pressure–temperature diagram and ln P vs. 1/T) and the variation in the amounts of CO_2 removed as a function of temperature, so as to study the reactivity and exothermicity effects in CO_2 capture testing using EDA. The temperature increased suddenly from the initial temperature (303 K) to point A (see Figure 4a). As previously discussed, the initial ΔT was due to the exothermicity of the CO_2 capture process using chemical solvents [6]. The combined effect of gas solubilization into the liquid phase and the chemical reaction between the solubilized gas and the liquid solution should increase the temperature in a CO_2 capture process using EDA. After point A, the heat released gradually dissipated in the same liquid solution and the reactor walls, producing continuous and gradual temperature decreases (segments AB and BC, see Figure 4b) until it stabilized again at the initial temperature. From that moment on, the reactor heating system maintained a constant temperature (segment CD). The reaction's thermal shock at the first moments of gas–liquid contact occurred without significant CO_2 consumption. The CO_2 capture was triggered after a minimal amount of CO_2 was absorbed into the liquid solutions (point B, see Figure 4c). Li et al. [53] proposed a reaction mechanism between EDA and CO_2, wherein the amino groups (–NH_2) react with CO_2 under the sufficient CO_2 conditions. Furthermore, it seems that this minimal amount of CO_2 (~10 mmol) was independent of the amine concentration, and could correspond to the "lean amine acid gas loading" in a typical sweetening process using alkanolamines as chemical solvents [32]. Momeni and Riahi [54] established that amines' chemical structure and nature are the most important parameters for CO_2 absorption purposes.

3.4. CO_2 Capture Using EDA: Kinetic and Thermodynamic Analysis

When analyzing the CO_2 loading behavior as a function of time (see Figure 3c), it was observed that the kinetic mechanism involved two steps: a rapid absorption step, and a slow diffusion step (Figure 5). This kinetic mechanism is similar to that reported for CO_2 adsorption processes [55]. Da Silva and Svendsen [56] commented that the two-step mechanism applies to the reaction between CO_2 and primary and secondary amines. Furthermore, Wai et al. [57] performed a kinetic and thermodynamic analysis of CO_2 capture for combustion gases using AMP–DETA (2-amino-2-methyl-1-propanol–diethylenetriamine) mixtures, and the trend was similar to what was observed in this work.

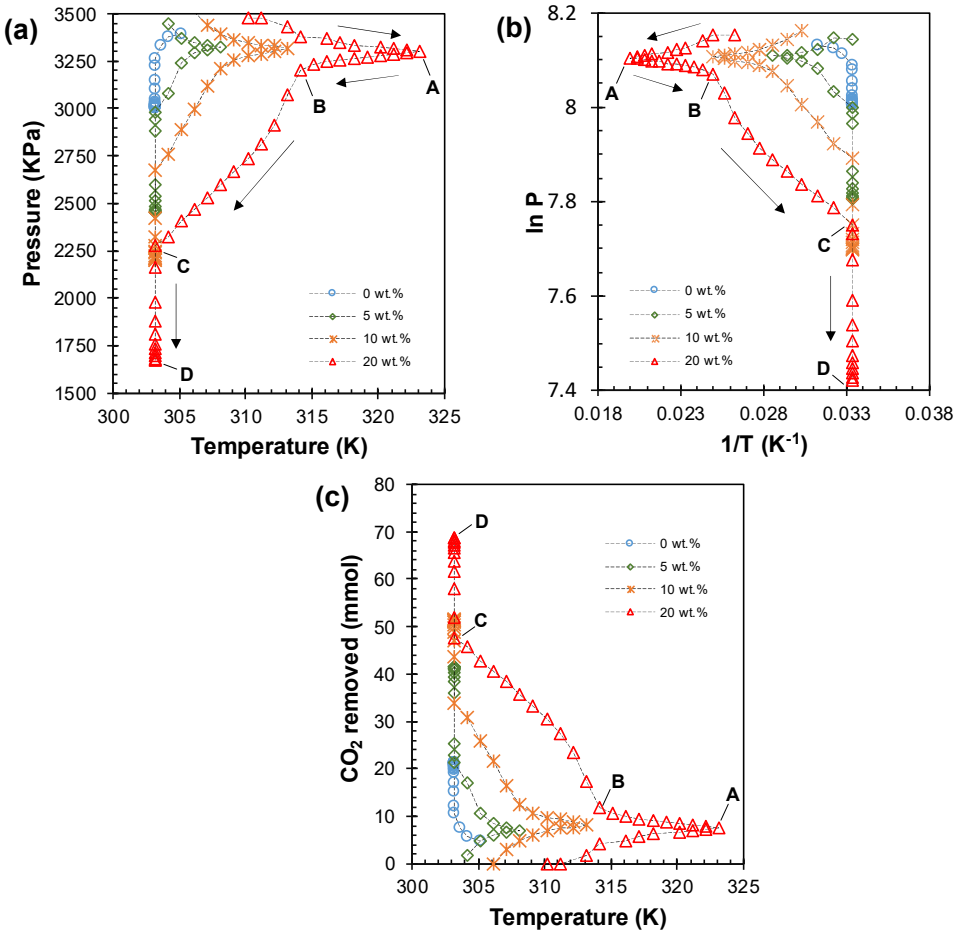

Figure 4. CO_2 capture using EDA—reaction exothermicity effects: (**a**) pressure–temperature diagram; (**b**) ln P vs. 1/T; (**c**) CO_2 removed vs. temperature.

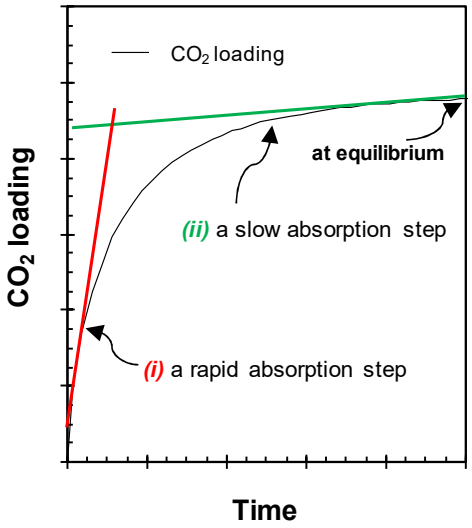

Figure 5. CO_2 capture using EDA: Kinetic mechanism proposal.

Equation (7) is the mathematical expression for the kinetic mechanism proposal. The first term corresponds to the CO_2 loading at equilibrium. The parameters (A_1, k_1, A_2, k_2)

of the time-dependent terms were determined by the least squares regression from the experimental data (CO_2 loading vs. time, Figure 3c).

$$n_{loading}^{CO_2}\Big|_{t=t} = n_{loading}^{CO_2}\Big|_{equil.} - A_1 \exp(-k_1 t) - A_2 \exp(-k_2 t) \quad (7)$$

Figure 6a shows the linear correspondence between CO_2 loading at equilibrium as a function of the EDA solution concentration. When EDA was not present in the liquid phase, the value of CO_2 loading at equilibrium coincided with the solubility of CO_2 in pure water. Increases in the EDA concentration produced an increased CO_2 loading. Muchan et al. [58] worked at atmospheric pressure with 15 KPa CO_2 (in nitrogen balance) using an aqueous EDA solution, while Singh [59] performed the evaluation of different amines for CO_2 capture using high-pressure systems. In both cases—at atmospheric pressure and at high pressure—the results were consistent with the linear tendency obtained in this work. This behavior suggests that the CO_2 loading at equilibrium conditions in aqueous EDA solutions is not a pressure-dependent parameter.

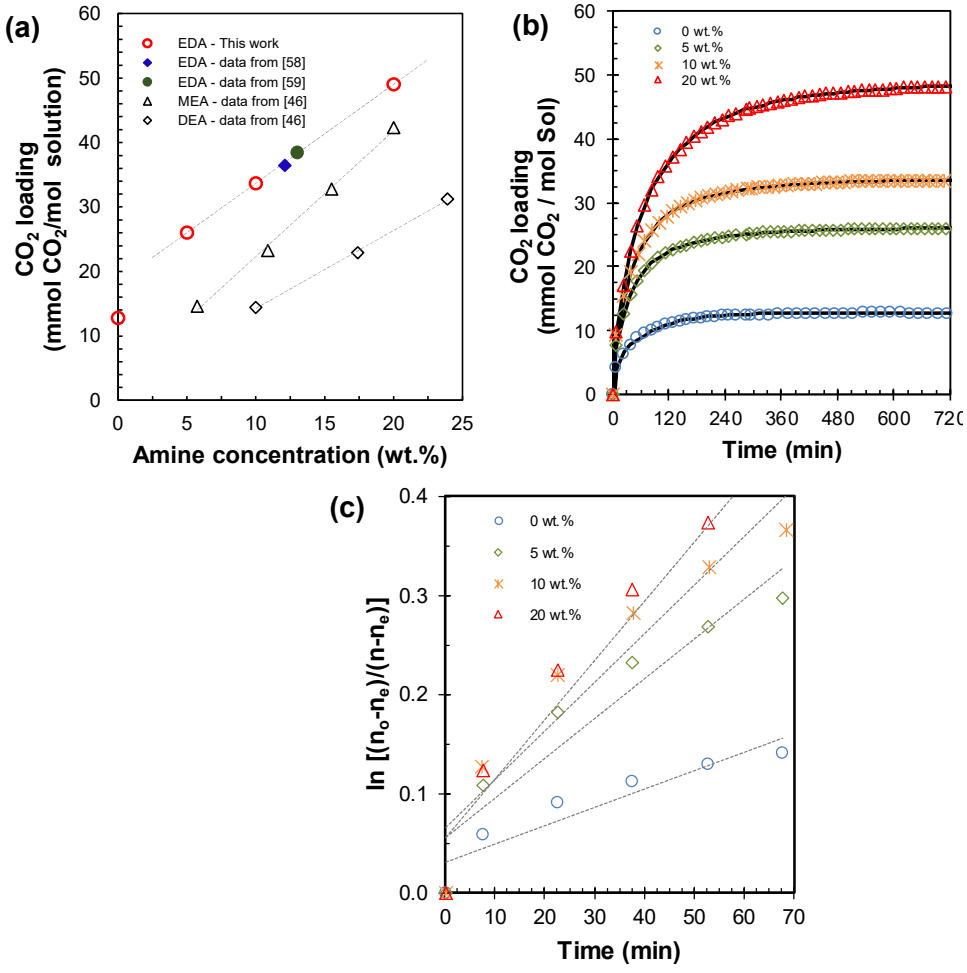

Figure 6. CO_2 capture using EDA—kinetic and thermodynamic analysis: (**a**) CO_2 loading at equilibrium vs. amine concentration; (**b**) CO_2 loading vs. time; (**c**) apparent absorption rate constant at different concentrations.

Moreover, Figure 6a shows the data on CO_2 loading for other amines (MEA, DEA) taken from [46]. Similarly, there was a linear relationship between the CO_2 loading and the amine concentration, as obtained for EDA in this work. Bernhardsen and Knuutila [60] reviewed potential amine solvents for the CO_2 absorption process, showing the linear dependence of CO_2 loading at equilibrium on the MEA concentration. MEA has a greater

absorption capacity than DEA, but EDA surpasses both in the concentration range studied. EDA has two amino groups that promote affinity and reactivity towards CO_2; however, this trend is not consistent with the results reported by Gomes et al. [61], where DEA and MEA achieved greater absorption capacity compared to EDA, possibly because the equilibrium conditions were not reached under their experimental setup.

Table 3 summarizes the kinetic model parameters for Equation (7). Figure 6b shows the experimental data fit according to the proposed equation. The average absolute deviation (AAD) was <1% for each EDA aqueous solution, showing that the CO_2 capture behavior obtained during the experimental testing adapted accurately to the kinetic mechanism, which involves two steps: a rapid absorption step, and a slow diffusion step. Li et al. [53] conducted CO_2 capture tests in a glass reactor, and obtained similar trends to our proposed mechanism.

Table 3. CO_2 capture using EDA: Kinetic model parameters for Equation (7).

EDA Conc. (wt.%)	Kinetic Data				AAD (%)
	A_1	$k_1 \times 10^3$	A_2	$k_2 \times 10^3$	
0	8.158	12.764	7.083	226.615	0.586
5	7.687	7.380	13.737	29.199	0.191
10	10.657	6.776	17.311	27.009	0.196
20	18.088	4.821	25.356	20.363	0.321

Finally, the damping-film theory model was applied to investigate the apparent absorption rate performance of an aqueous EDA solution using Equation (4) at the rapid absorption step. Slopes of the constant rate (k) of aqueous solutions of EDA are shown in Figure 6c. The apparent absorption rate constant of aqueous EDA solutions was much higher than that of pure water, with a value of 0.0019 min^{-1}. It was also observed that EDA significantly intensified the CO_2 absorption performance of aqueous solutions, resulting in k values of 0.0040 min^{-1}, 0.0049 min^{-1}, and 0.0060 min^{-1} for EDA concentrations of 5, 10, and 20 wt.%, respectively. Note that in the initial minutes (<10 min), the CO_2 absorption rate was higher for 10 wt.% EDA solutions, consistent with the initial CO_2 capture rate values (see dn/dt data in Table 2). The addition of EDA accelerated the absorption performance of the CO_2-trapping chemical solvent within the investigated timeframe. The increased absorption performance in aqueous EDA solutions was due to the chemical absorption of CO_2 into aqueous solutions of diamine at high pressure taking less time to absorb more CO_2 molecules than pure water.

4. Summary and Outlook

In this work, an experimental setup was installed and commissioned for CO_2 capture testing, using EDA as a chemical solvent, with the main distinction being the pure CO_2 bubbling directly into the liquid phase so as to guarantee intimate contact between the gas and the liquid from the first instants of the experiments. Initial testing of the solubility of CO_2 in water allowed the validation of the experimental setup and the proposed methodology, demonstrating that it was possible to reach equilibrium conditions in short times (<4 h) using a non-stirred system. CO_2 capture testing was carried out using EDA aqueous solutions at different concentrations (0, 5, 10, and 20 wt.% in amine). The addition of EDA accelerated the CO_2 capture performance, and the drop in pressure was proportional to the amine concentration. For the 20 wt.% amine solution, the gas consumption represented a drop in pressure of ~50% from the initial pressure. During the initial minutes of the CO_2 capture process, sudden temperature increases were observed as a result of the exothermic reaction between the CO_2 and the EDA aqueous solutions. The maximum value reached was ~324 K for the 20 wt.% amine solution, representing a $\Delta T = 21$ K.

The CO_2 capture was triggered after the absorption of a minimal amount of CO_2 (~10 mmol) into the liquid solutions. There was a linear relationship between the CO_2 loading and the EDA concentration at equilibrium conditions. Compared with other

alkanolamines commonly used as chemical solvents, EDA had a higher CO_2 absorption capacity than MEA and DEA in the concentration range studied. EDA has two amino groups that promote affinity and reactivity towards CO_2. A kinetic model involving two steps (a rapid absorption step and a slow diffusion step) was proposed to ascertain the CO_2 loading at equilibrium, the CO_2 loading as a function of time, and the apparent absorption rate. The apparent absorption rate constants of aqueous EDA solutions were higher than those for pure water, resulting in a k of 0.0060 min^{-1} for 20 wt.% EDA solutions.

Subsequent characterization studies of saturated amines will allow us to identify and quantify reaction products for the CO_2–EDA–water system. Additionally, amine regeneration testing will be performed through absorption/desorption cycles in order to ascertain the energy demands of the CO_2 capture process using EDA, as well as the limit operating temperature in the stripping process. CO_2 capture at different temperatures will allow us to conduct absorption enthalpy analyses using EDA as a chemical solvent.

Author Contributions: Conceptualization, J.A.V. and M.R.; methodology, A.V. and M.R.; investigation, J.A.V., A.P.-C., A.V. and M.R.; writing—original draft preparation, J.A.V. and M.R.; writing—review and editing, A.P.-C. and M.R.; funding acquisition, A.V. All authors have read and agreed to the published version of the manuscript.

Funding: This research was funded by SENESCYT, Ecuador (grant number PIC-18-INE-YACHAY-001), and the Yachay Tech University (project number CHEM19-02).

Institutional Review Board Statement: Not applicable.

Informed Consent Statement: Not applicable.

Data Availability Statement: Not applicable.

Acknowledgments: The support of Daniela Navas (laboratory technician at Yachay Tech University) is appreciated.

Conflicts of Interest: The authors declare no conflict of interest.

Appendix A. Mole Number in EDA Aqueous Solutions

A polynomial adjustment (Figure A1) of the experimental data reported by Egorov et al. [37] was carried out to estimate the density of aqueous EDA solutions at different concentrations (<30 wt.% in amine).

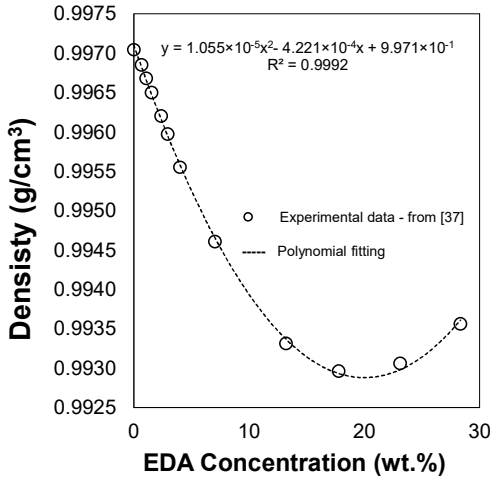

Figure A1. Density vs. EDA solution concentrations.

Then, the mole numbers of amine (n_{EDA}), water (n_{H_2O}), and total moles in the liquid phase (n_{liquid}) initially present in each of the EDA aqueous solutions (Table A1) were

calculated from the solutions' density and the molecular weight of EDA and water. A fixed volume (30 ± 0.2 cm^3) of the amine solutions was used in the CO_2 capture testing.

Table A1. Mole numbers in EDA aqueous solutions.

EDA Conc. (wt.%)	Density (g/cm^3)	n_{EDA} (mole)	n_{H_2O} (mole)	n_{liquid} (mole)
0	0.997	-	1.660	1.660
5	0.995	0.025	1.574	1.599
10	0.994	0.050	1.490	1.540
20	0.993	0.099	1.323	1.422

References

1. International Energy Agency. *Global Energy Review 2020*; IEA: Paris, France, 2020. Available online: https://www.iea.org/reports/global-energy-review-2020 (accessed on 1 September 2021).
2. Center for Climate and Energy Solutions. *Global Emissions*; C2ES: Arlington, TX, USA, 2020. Available online: https://www.c2es.org/content/international-emissions (accessed on 1 September 2021).
3. United Nations Framework Convention on Climate Change. The Paris Agreement. Adopted 12 December 2015. Available online: https://www.un.org/en/climatechange/paris-agreement (accessed on 1 September 2021).
4. Intergovernmental Panel on Climate Change. *IPCC Special Report on Carbon Dioxide Capture and Storage*; Cambridge University Press: Cambridge, UK, 2005; p. 431. ISBN 978-0-521-86336-0.
5. Liang, Z.; Fu, K.; Idem, R.; Tontiwachwuthikul, P. Review on current advances, future challenges and consideration issues for post-combustion CO_2 capture using amine-based absorbents. *Chin. J. Chem. Eng.* **2016**, *24*, 278–288. [CrossRef]
6. Kohl, A.; Nielsen, R. Chapter 2-alkanolamines for hydrogen sulfide and carbon dioxide removal. In *Gas Purification*, 5th ed.; Gulf Professional Publishing: Houston, TX, USA, 1997; pp. 40–186. [CrossRef]
7. Nwaoha, C.; Beaulieu, M.; Tontiwachwuthikul, P.; Gibson, M. Techno-economic analysis of CO_2 capture from a 1.2 million MTPA cement plant using AMP-PZ-MEA blend. *Int. J. Greenh. Gas Control* **2018**, *78*, 400–412. [CrossRef]
8. Rochelle, G. Amine scrubbing for CO_2 capture. *Science* **2009**, *325*, 1652–1654. [CrossRef]
9. Feron, P.; Cousins, A.; Jiang, K.; Zhai, R.; Garcia, M. An update of the benchmark post-combustion CO_2-capture technology. *Fuel* **2020**, *273*, 117776. [CrossRef]
10. Adu, E.; Zhang, Y.D.; Liu, D.; Tontiwachwuthikul, P. Parametric process design and economic analysis of post-combustion CO_2 capture and compression for coal- and natural gas-fired power plants. *Energies* **2020**, *13*, 2519. [CrossRef]
11. Garba, Z.; Galadima, A. Carbon capture and storage (CCS) technology: Challenges to implementation. In *Encyclopedia of Renewable and Sustainable Materials*, 1st ed.; Hashmi, S., Chudhury, I., Eds.; Elsevier: New York, NY, USA, 2020; Volume 3, pp. 291–299. [CrossRef]
12. Ishaq, H.; Ali, U.; Sher, F.; Anus, M.; Imran, M. Process analysis of improved process modifications for ammonia-based post-combustion CO_2 capture. *J. Environ. Chem. Eng.* **2021**, *9*, 104928. [CrossRef]
13. Nwaoha, C.; Tontiwachwuthikul, P.; Benamor, A. CO_2 capture from lime kiln using AMP-DA2MP amine solvent blend: A pilot plant study. *J. Environ. Chem. Eng.* **2018**, *6*, 7102–7110. [CrossRef]
14. Raznahan, M.; Riahi, S.; Mousavi, S. A simple, robust and efficient structural model to predict CO_2 absorption for different amine solutions: Concern to design new amine compounds. *J. Environ. Chem. Eng.* **2020**, *8*, 104572. [CrossRef]
15. Borhani, T.; Wang, M. Role of solvents in CO_2 capture processes: The review of selection and design methods. *Renew. Sustain. Energy Rev.* **2019**, *114*, 109299. [CrossRef]
16. Ume, C.; Ozturk, M.; Alper, E. Kinetics of CO_2 absorption by a blended aqueous amine solution. *Chem. Eng. Technol.* **2012**, *35*, 464–468. [CrossRef]
17. Lestari, I.; Rahayu, D.; Nurani, D.; Krisnandi, Y.; Budianto, E. Ethylenediamine-derived imidazoline synthesis using MAOS (Microwave Assisted Organic Synthesis) method. *AIP Conf. Proc.* **2019**, *2168*, 020066. [CrossRef]
18. Li, J.; Henni, A.; Tontiwachwuthikul, P. Reaction kinetics of CO_2 in aqueous ethylenediamine, ethyl ethanolamine, and diethyl monoethanolamine solutions in the temperature range of 298-313 K, using the stopped-flow technique. *Ind. Eng. Chem. Res.* **2007**, *46*, 4426–4434. [CrossRef]
19. Salvi, A.; Vaidya, P.; Kenig, E. Kinetics of carbon dioxide removal by ethylenediamine and diethylenetriamine in aqueous solutions. *Can. J. Chem. Eng.* **2014**, *92*, 2021–2028. [CrossRef]
20. Zhou, S.; Chen, X.; Nguyen, T.; Voice, A.; Rochelle, G. Aqueous ethylenediamine for CO_2 capture. *ChemSusChem* **2010**, *3*, 913–918. [CrossRef]
21. Hafizi, A.; Mokari, M.; Khalifeh, R.; Farsi, M.; Raphimpour, M. Improving the CO_2 solubility in aqueous mixture of MDEA and different polyamine promoters: The effects of primary and secondary functional groups. *J. Mol. Liq.* **2020**, *297*, 111803. [CrossRef]

22. Kumar, S.; Padhan, R.; Mondal, M. Equilibrium solubility measurement and modeling of CO_2 absorption in aqueous blend of 2-(diethyl amino) ethanol and ethylenediamine. *J. Chem. Eng. Data* **2020**, *65*, 523–531. [CrossRef]
23. Nakhjiri, A.; Heydarinasab, A. Computational simulation and theoretical modeling of CO_2 separation using EDA, PZEA and PS absorbents inside the hollow fiber membrane contactor. *J. Ind. Eng. Chem.* **2019**, *78*, 106–115. [CrossRef]
24. Ciftja, A.; Hartono, A.; Svendsen, H. Carbamate formation in aqueous—diamine—CO_2 systems. *Energy Procedia* **2013**, *37*, 1605–1612. [CrossRef]
25. Da Silva, E.; Svendsen, H. Computational chemistry study of reactions, equilibrium and kinetics of chemical CO_2 absorption. *Int. J. Greenh. Gas Control* **2007**, *1*, 151–157. [CrossRef]
26. Thompson, J.; Richburg, H.; Liu, K. Thermal degradation pathways of aqueous diamine CO_2 capture solvents. *Energy Procedia* **2017**, *114*, 2030–2038. [CrossRef]
27. Hikita, H.; Asai, S.; Ishikawa, H.; Honda, M. The kinetics of reactions of carbon dioxide with monoisopropanolamine, diglycolamine and ethylenediamine by a rapid mixing method. *Chem. Eng. J.* **1977**, *14*, 27–30. [CrossRef]
28. Jensen, A.; Christensen, R. Studies on carbamates. XI. The carbamate of ethylenediamine. *Acta Chem. Scand.* **1955**, *9*, 486–492. [CrossRef]
29. Gaines, G. The structure of (ammonioethyl)carbamate in solution. *J. Org. Chem.* **1985**, *50*, 410–411. [CrossRef]
30. Lee, B.; Lee, K.; Lim, B.; Cho, J.; Nam, W.; Hur, N. Direct synthesis of imines via solid state reactions of carbamates with aldehydes. *Adv. Synth. Catal.* **2013**, *355*, 389–394. [CrossRef]
31. Feng, Z.; Cheng-Gang, F.; You-Ting, W.; Yuan-Tao, W.; Ai-Min, L.; Zhi-Bing, Z. Absorption of CO_2 in the aqueous solutions of functionalized ionic liquids and MDEA. *Chem. Eng. J.* **2010**, *160*, 691–697. [CrossRef]
32. Khan, S.; Hailegiorgis, S.; Man, Z.; Garg, S.; Shariff, A.; Farrukh, S.; Ayoub, M.; Ghaedi, H. High-pressure absorption study of CO_2 in aqueous N-methyldiethanolamine (MDEA) and MDEA-piperazine (PZ)-1-butyl-3-methylimidazolium trifluoromethanesulfonate [bmim][OTf] hybrid solvents. *J. Mol. Liq.* **2018**, *249*, 1236–1244. [CrossRef]
33. Kidnay, A.; Parrish, W.; McCartney, G. *Fundamentals of Natural Gas Processing*, 3rd ed.; CRC Press—Taylor & Francis Group: Boca Raton, FL, USA, 2020; pp. 217–248. ISBN 978-1-138-61279-2.
34. Abro, M.; Yu, L.; Yu, G.; Chen, X.; Qazi, A. Experimental investigation of hydrodynamic parameters and bubble characteristics in CO_2 absorption column using pure ionic liquid and binary mixtures: Effect of porous sparger and operating conditions. *Chem. Eng. Sci.* **2021**, *229*, 116041. [CrossRef]
35. Zhong, H.; Fujii, K.; Nakano, Y.; Jin, F. Effect of CO_2 bubbling into aqueous solutions used for electrochemical reduction of CO_2 for energy conversion and storage. *J. Phys. Chem. C* **2015**, *119*, 55–61. [CrossRef]
36. Peng, D.; Robinson, D. A new two-constant equation of state. *Ind. Eng. Chem. Fundam.* **1976**, *15*, 59–64. [CrossRef]
37. Egorov, G.; Makarov, D.; Kolker, A. Volume properties of liquid mixture of {water (1) + ethylenediamine (2)} over the temperature range from 274.15 to 333.15 K at atmospheric pressure. *Thermochim. Acta* **2016**, *639*, 148–159. [CrossRef]
38. Fogler, S. *Elements of Chemical Reaction Engineering*, 3rd ed.; Prentice-Hall India: New Delhi, India, 2004; pp. 223–281. ISBN 81-203-2234-7.
39. Ricaurte, M.; Torré, J.-P.; Asbai, A.; Broseta, D.; Dicharry, C. Experimental data, modeling, and correlation of carbon dioxide solubility in aqueous solutions containing low concentrations of clathrate hydrate promoters: Application to CO_2-CH_4 gas mixtures. *Ind. Eng. Chem. Res.* **2012**, *51*, 3157–3169. [CrossRef]
40. Farajzadeh, R.; Barati, A.; Delil, H.; Bruining, J.; Zitha, P. Mass transfer of CO_2 into water and surfactant solutions. *Pet. Sci. Technol.* **2007**, *25*, 1493–1511. [CrossRef]
41. Diamond, L.; Akinfiev, N. Solubility of CO_2 in water from −1.5 to 100 °C and from 0.1 to 100 MPa: Evaluation of literature data and thermodynamic modelling. *Fluid Ph. Equilibria* **2003**, *208*, 265–290. [CrossRef]
42. Hemmati, A.; Farahzad, R.; Surendar, A.; Aminahmadi, B. Validation of mass transfer and liquid holdup correlations for CO_2 absorption process with methyldiethanolamine solvent and piperazine as an activator. *Process Saf. Environ. Prot.* **2019**, *126*, 214–222. [CrossRef]
43. Bourne, J.; von Stockar, U.; Coggan, G. Gas absorption with heat effects. Experimental results. *Ind. Eng. Chem. Process. Des. Dev.* **1974**, *13*, 124–132. [CrossRef]
44. Green, D.; Perry, R. *Perry's Chemical Engineers' Handbook*, 8th ed.; McGraw-Hill: New York, NY, USA, 2008; pp. 14-1–14-129. ISBN 0-07-159313-6.
45. Hikita, H.; Ishikawa, H.; Murakami, T.; Ishii, T. Densities, viscosities and amine diffusivities of aqueous MIPA, DIPA, DGA and EDA solutions. *J. Chem. Eng. Jpn.* **1981**, *14*, 411–413. [CrossRef]
46. Fan, W.; Lui, Y.; Wang, F. Detailed experimental study on the performance of monoethanolamine, diethanolamine, and diethylenetriamine at absorption/regeneration conditions. *J. Clean. Prod.* **2016**, *125*, 296–308. [CrossRef]
47. Bui, M.; Tait, P.; Lucquiaud, M.; Mac Dowell, N. Dynamic operation and modelling of amine-based CO_2 capture at pilot scale. *Int. J. Greenh. Gas Control* **2018**, *79*, 134–153. [CrossRef]
48. Rabensteiner, M.; Kinger, G.; Koller, M.; Gronald, G.; Hochenauer, C. Pilot plant study of ethylenediamine as a solvent for post combustion carbon dioxide capture and comparison to monoethanolamine. *Int. J. Greenh. Gas Control* **2014**, *27*, 1–14. [CrossRef]
49. Stec, M.; Tatarczuk, A.; Więcław-Solny, L.; Krótki, A.; Ściążko, M.; Tokarski, S. Pilot plant results for advanced CO_2 capture process using amine scrubbing at the Jaworzno II Power Plant in Poland. *Fuel* **2015**, *151*, 50–56. [CrossRef]

50. Hemmati, A.; Rashidi, H. Mass transfer investigation and operational sensitivity analysis of amine-based industrial CO_2 capture plant. *Chin. J. Chem. Eng.* **2019**, *27*, 534–543. [CrossRef]
51. Li, F.; Hemmati, A.; Rashidi, H. Industrial CO_2 absorption into methyldiethanolamine/piperazine in place of monoethanolamine in the absorption column. *Process Saf. Environ. Prot.* **2020**, *142*, 83–91. [CrossRef]
52. Vega, F.; Baena-Moreno, F.; Gallego, L.; Portillo, E.; Navarrete, B. Current status of CO_2 chemical absorption research applied to CCS: Towards full deployment at industrial scale. *Appl. Energy* **2020**, *260*, 114313. [CrossRef]
53. Li, Y.; Cheng, J.; Hu, L.; Liu, N.; Zhou, J.; Cen, K. Regulating crystal structures of EDA-carbamates in solid-liquid phase changing CO_2 capture solutions. *Fuel* **2019**, *252*, 47–54. [CrossRef]
54. Momeni, M.; Riahi, S. An investigation into the relationship between molecular structure and rich/lean loading of linear amine-based CO_2 absorbents. *Int. J. Greenh. Gas Control* **2015**, *61*, 157–164. [CrossRef]
55. Loganathan, S.; Tikmani, M.; Mishra, A.; Kumar, A. Amine tethered pore-expanded MCM-41 for CO_2 capture: Experimental, isotherm and kinetic modeling studies. *Chem. Eng. J.* **2016**, *303*, 89–99. [CrossRef]
56. Da Silva, E.; Svendsen, H. Comment on "Reaction kinetics of CO_2 in aqueous ethylenediamine, ethyl ethanolamine, and diethyl monoethanolamine solutions in the temperature range of 298-313 K, using the stopped-flow technique". *Ind. Eng. Chem. Res.* **2008**, *47*, 990. [CrossRef]
57. Wai, S.; Nwaoha, C.; Saiwan, C.; Idem, R.; Supap, T. Absorption heat, solubility, absorption and desorption rates, cyclic capacity, heat duty, and absorption kinetic modeling of AMP-DETA blend for post-combustion CO_2 capture. *Sep. Purif. Technol.* **2018**, *94*, 89–95. [CrossRef]
58. Muchan, P.; Narku-Tetteh, J.; Saiwan, C.; Idem, R.; Supap, T. Effect of number of amine groups in aqueous polyamine solution on carbon dioxide (CO_2) capture activities. *Sep. Purif. Technol.* **2017**, *184*, 128–134. [CrossRef]
59. Singh, P. Amine Base Solvent for CO_2 Absorption "from Molecular Structure to Process". Ph.D. Thesis, University of Twente, Enschede, The Netherlands, 2011. [CrossRef]
60. Bernhardsen, I.; Knuutila, H. A review of potential amine solvents for CO_2 absorption process: Absorption capacity, cyclic capacity and pKa. *Int. J. Greenh. Gas Control* **2017**, *61*, 27–48. [CrossRef]
61. Gomes, J.; Santos, S.; Bordado, J. Choosing amine-based absorbents for CO_2 capture. *Environ. Technol.* **2015**, *36*, 19–25. [CrossRef] [PubMed]